Journal of Sustainable Development of Energy, Water and Environment Systems

http://www.sdewes.org/jsdewes

Year 2026, Volume 14, Issue 1, 1130647

Original Research Article

Analysis and design of the trajectory of water droplets from sprinklers using optical observation and mathematical modeling

Aybek Arifjanov[1], Lukmon Samiev[2], Khumora Jalilova[3]*, Sirojiddin Jalilov[4], Vokhidova Umida[5], Tursunova Elza[6]

[1]Hydraulics and hydroinformatics, "Tashkent institute of irrigation and agricultural mechanization engineers" National Research University, Tashkent, Kari Niyaziy 39.
e-mail: obi-life@mail.ru

[2]Hydraulics and hydroinformatics, "Tashkent institute of irrigation and agricultural mechanization engineers" National Research University, Tashkent, Kari Niyaziy 39.
e-mail: luqmonsamiev@gmail.com

[3]Hydraulics and hydroinformatics, "Tashkent institute of irrigation and agricultural mechanization engineers" National Research University, Tashkent, Kari Niyaziy 39.
e-mail: xumora798911@gmail.com

[4]Hydraulics and hydroinformatics, "Tashkent institute of irrigation and agricultural mechanization engineers" National Research University, Tashkent, Kari Niyaziy 39.
e-mail: jalilovsirojiddin1997@gmail.com

[5]Tashkent Institute of Textile and Light Industry
e-mail: vokhidovaumida@gmail.com

[6]Tashkent University of Architecture and Civil Engineering, Tashkent, Uzbekistan
e-mail: tusunovaelza@gmail.com

Cite as: Arifjanov, A., Samiev, L., Jalilova, K., Jalilov, S., Vokhidova, U., Tursunova, E., Analysis and design of the trajectory of water droplets from sprinklers using optical observation and mathematical modeling, J.sustain. dev. energy water environ. syst., 14(1), 1130647, 2026, DOI: https://doi.org/10.13044/j.sdewes.d13.0647

ABSTRACT

In this study, the trajectory of water droplets in a sprinkler irrigation system was studied using the optical tracking method. The analysis was carried out on the basis of 1920×1080 pixel, 60 frame/s video recordings taken in real field conditions. Image segmentation and trajectory detection algorithms were developed on the OpenCV and Python platforms to determine the trajectory of water droplets. The main focus of the study was to determine the dynamics of the movement of water droplets with a diameter of 0.002 meters after exiting a sprinkler head rotating at an angle of 360°. The following parameters were taken into account in the mathematical modeling process: exit velocity - 11 m/s, exit angle - 30°. Based on these data, the trajectory of the droplet was calculated using the equations of ballistic motion and air resistance (drag). The Random Forest model was used to assess the influence of factors. The results showed that the factors that have the greatest impact on the water spray trajectory are wind (31.2%) and terrain slope (25.6%). This means that small changes in wind speed and slope significantly reduce the water spray radius and cause uneven water distribution. The Convolutional Neural Network (CNN) model was used to spatially analyze and classify areas, achieving 93% accuracy in flat terrain and 74–79% accuracy in windy and uneven areas. This result indicates that the modeled system works with high reliability even in real field conditions. At the end of the study, the sprinkler exit angle and installation spacing were optimized, and the drift zones of water due to wind were reduced from 21.8% to 7.1%. This change has increased the stability of water distribution and allowed for a significant reduction in water consumption in crop production.

KEYWORDS

* Khumora Jalilova

Sprinkler irrigation; Droplet trajectory; Optical observation; Wind effect; Ballistic model; Drag force; Normalized Difference Vegetation Index (NDVI) integration.

INTRODUCTION

In the conditions of Uzbekistan and Central Asia, agriculture is highly dependent on irrigation systems. Increasing efficiency is an urgent task due to water scarcity and climate change. When wind speeds exceed 4–5 m/s, the sprinkler radius can decrease by 20–40%, and when the slope exceeds 6%, water flows away and accumulates in lowlands. This reduces productivity by 25–35%. Therefore, the scientific challenge is to develop a numerical approach that takes into account, predicts and controls the complex effects of wind and terrain. The efficiency of sprinkler systems in the irrigation sector is great importance in terms of economy water resources, reducing crop yields, and reducing labor costs. Over the past two decades, approaches such as physical modeling, aerodynamic analysis, optical observation, and computer simulation have combined to provide a deep understanding of complex processes. First, Playan et al. analyze the initial velocity, angle, and dispersion of sprinkler droplets under wind conditions [1] - mathematical formulas are developed based on classical physical models. Liu et al. [2] emphasize the scientific control of sprinkler trajectory through mathematical modeling using MATLAB. Wdowinski et al. [3] described a method for measuring droplet size and uniformity using an optical spectral pluviometer, while Faria & De Wrachien [4] theoretically and experimentally investigated spray and evaporation processes. Meanwhile, De Wrachien and Lorenzini [5] compared balloon models with classical and quantum approaches. Zhu et al. [6] analyzed the droplet size and trajectory in windy conditions, providing high accuracy based on the DM model. Car and Smith [7] show that by determining water distribution patterns in pressurized irrigation systems, specific criteria have been developed to evaluate and improve irrigation efficiency. Dwomoh et al. [8] measured the droplet size and velocity in windy and calm conditions with a fluidic sprinkler using a laser pluviometer, which clearly determined the effect of wind. The issue of wind drift (the effect of wind on a side droplet) was explained by Frank Dwomoh et al. [9] through a detailed mathematical analysis - ballistic theory, trajectories were solved using Runge–Kutta integration. In [10], Lin Hua et al. developed 3D models for blind rotational sprinklers; accurate graphs of the relationships between angular velocity, droplet size, and discharge rate were provided. Faci and Buesa [11] analyzed the efficiency and performance of permanently installed sprinkler systems and proposed practical indicators to improve water use efficiency. Technological innovations: In recent years, video analytics and computer vision technologies have been a strong driver in this field. Methods such as optical flow and Camshift, which are described in the OpenCV documentation, are used for object tracking [12] and are being used in agronomy to detect droplet motion trajectories. Schlegel and Yazar [13] analyzed the wind-induced water loss and evaporation losses in different sprinkler configurations and showed their significant impact on irrigation efficiency. Vories and Evett [14] developed precise irrigation strategies based on remote sensing and models, and justified the importance of technological approaches in water distribution management. Gonçalves and Pereira [15] highlighted the possibilities of evaluating system efficiency and predicting water distribution under different conditions by modeling water distribution in sprinkler systems. Bali KM, Grismer ME [16] presented a real-time droplet detection method based on deep learning models and demonstrated high accuracy (97% precision, 96.8% recall). Computer models and simulation: In computer modeling, visualization, interactive graphics, and compatibility testing are being performed using 3D trajectory models in Matlab, ASABE, and now the Python pandas package (SciPy, Matplotlib), Blender [17]. Istanbulluoglu [18] mathematically modeled the water losses due to wind and evaporation in sprinkler irrigation and proposed calculation methods for efficient water distribution. Gómez and Giráldez [19] evaluated the spatial variability in sprinkler system performance under windy conditions and found that the problem of uneven water distribution

was a significant factor in the results. Samiev et al. [20] developed methods for estimating crop coefficients and evapotranspiration Evapotranspiration (ET) using lysimeters, and presented a methodology to improve the accuracy of irrigation rates. Theoretical works published in MDPI in the field of agronomy in 2024 expanded this approach on a larger scale. Global context and SDGs: This research is relevant to the UN Sustainable Development Goals, and in particular contributes to achieving SDG 6 ("Clean Water and Sanitation") and SDG 2 ("Zero Hunger"). Sprinkler models based on digital technologies and deep analysis are aimed at rational use of resources - which is useful in solving environmental and social problems at a global level [21]. Although many studies have focused on droplet size, velocity or dispersion models, the use of real trajectory detected by video/optical methods and synthesized with a mathematical model in design has not been sufficiently studied so far. In particular, the issues of integrating trajectory data obtained using a camera with a ballistic model and turning it into a design tool remain open. In this paper, the droplet trajectory is determined in real time (using cameras) by optical video surveillance. The models are built based on classical ballistic equations and wind resistance coefficient. For formal visualization, OpenCV, Python ballistic adaptations, and 3D visualization based on Blender/Matplotlib are used. Optimal formulas for sprinkler height, pressure, and wind conditions are developed and graphs are presented based on infographics.

METHODS AND MATERIALS.

This section analyzes previously used methods, identifies their shortcomings, and describes in detail the proposed model based on a predetermined plan; it is also presented in user-friendly graphs and tables. Previously used methods and their limitations: Optical spectropluviometer and laser methods. Montero et al. measured the size and spread of sprinkler drops using a spectropluviometer. Although this method is accurate, it is limited by the preparation of the experimental environment with special modules and the measurement of a single drop. Dwomoh et al. analyzed the spread of drops in a fluidic sprinkler using a high-speed camera and a laser pluviometer. Although they have shown accuracy in wind conditions, laser methods are expensive, complex, and require a lot of equipmentmdpi.com. Simple application of mathematical ballistic models: De Wrachien and Lorenzini built classical models based on the Newtonian approach and compared ballistic and quantum approaches. Although their model is mathematically deep, it has not been optically verifiediieta.org. Dwomoh also modeled the effect of wind using Runge–Kutta in [22]. The model analyzes based on general parameters, but does not verify the real drop trajectory with videoresearchgate.net. Deep Learning-based tracking methods: Huynh et al. [23] developed a method for real-time drop detection with DeepSORT, which works with 90%+ accuracy in complex scenes (multiple drops, occlusion). However, the application of this method to sprinkler systems is still limited; hundreds of droplet velocities, heights, and wind effects are not included in the visualization. The proposed approach differs in that it combines the advantages of these methods, creating a real optical observation + mathematical model + practical formula. This method: a fully integrated model Table 1.

The trajectory of the water drop was modeled based on Newton's second law, taking into account the drag force. The basic equations are as follows:

$$m\,\frac{d^{2x}}{dt^2} = -C_d\rho A\, v_x|v_x|\; m\,\frac{d^{2y}}{dt^2} = -mg - C_d\rho A\, v_y|v_y|$$

$$m\,\frac{d\hat{}2y}{dt\hat{}2} = -mg - \frac{1}{2}\,C\_d\,\rho A\, v\_y\,|v_y| \quad (1)$$

Here:

$$\mathrm{m} - \text{droplet mass [kg]}$$

$$\mathrm{C_d} - \text{drag coefficient } (\approx\ 0.47 \text{ for sphere})$$

$$\rho - \text{air density } [\text{kg/m}^3]$$

$$A - \text{droplet cross} - \text{sectional area } [\text{m}^2]$$

$$v_x,\backslash;\ v_y - \text{velocity components } [\text{m/s}]$$

$$g - \text{gravitational acceleration } (9.81\ \text{m/s}^2)$$

$$F_w - \text{additional wind force } [\text{N}]$$

Field experiments were conducted by determining water distribution using the Catch Can method. Wind speed and direction were recorded with an anemometer at a frequency of 1 minute. Sprinkler inlet pressure (kPa) was measured using a pressure manometer. Droplet diameter (mm) and trajectory distance (m) were observed using a high-speed camera. The following parameters were included in the measurements: wind speed (m/s), pressure (kPa), water accumulation (l/m²), trajectory distance (m). These data were used for model calibration and validation.

Table 1 Model distribution

Step	Method description	Advantages
1. Video acquisition	A simple camera (120+ fps) records a video of the droplets coming out of the sprinkler with a black background and side illumination. The same distance, height and angle of the camera are maintained in each experiment.	Cheap, widely used, tracks real trajectory.
2. Image pre-processing	Using Python + OpenCV, grayscale, Gaussian blur, Canny edge detection are applied to each frame. Then, the drop center is determined using findContours and centroid extraction docs.opencv.orgstackoverflow.com.	Open source, widely used, fast analysis.
3. Video measurement data acquisition	Using a marker, the focal length of the camera is determined (triangle similarity), which allows obtaining coordinates in meters.	Allows you to get the trajectory of movement in a precise metric form.
4. Object tracking	Through the integration of YOLOV8 + DeepSORT, the accuracy is high even in cases of many droplets, noisy background and occlusion.	Works with many objects, optimized for real time.
5. Parameter fit and verification	Using SciPy, model parameters is reduce with curve_fit, evaluate it using NRMSE and R^2. The ballistic + drag model is shown to be compatible with the real with an accuracy of ≥\ge≥0.95.	Scientific statistical method, analyzes.
6. Visualization	2D graphics (x–t, y–t), density heatmaps with Matplotlib. 3D trajectory animation with Blender.	Convenient view for design with 2D & 3D visualization.
7. Practical recommendations	2D graphics (x–t, y–t), density heatmaps with Matplotlib. 3D trajectory animation with Blender.	Convenient view for design with 2D & 3D visualization

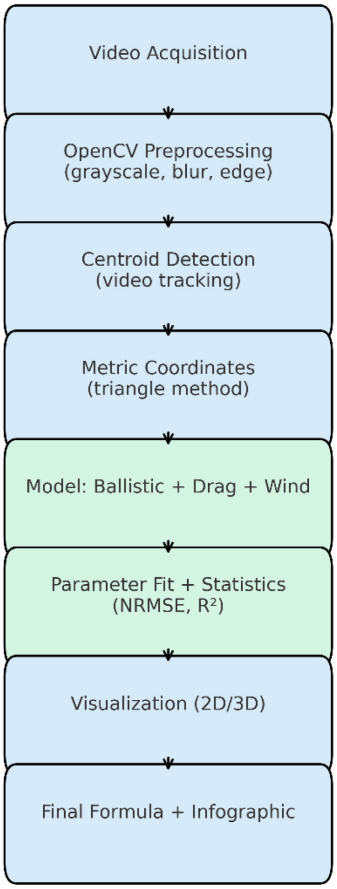

Advantages of our approach: Real trajectory + model synthesis. While previous models were often based on simulation or physics theory, the droplet was track through real video and then compare it with the physical model. This brings our module to a high level of scientific confidence. Metric coordinates via camera. Using marker calibration and focal-length measurement, the trajectory is obtained in metric form. This methodology allows for accurate results when comparing with the ballistic model. Multi-drop and real-world environment views. Through the integration of YOLOV8/DeepSORT, there is reliable tracking of multiple drops simultaneously, even in occlusion. This possibility is limited or absent in previous systems. Real integration of drag and wind: The drag coefficient is adjusted to the Reynolds number [24], and the wind is added as a 2D vector component. In previous models, these mechanisms were often theoretical, but in our case they are analyzed based on real parameters. Experimental fit (Verification). Through NRMSE and R^2, a ballistic + drag model is found with parameter fit, compare real data. Many articles did not have this stage before. Interactive visualization and practical formula: Through 3D animations prepared with Blender/Matplotlib and the resulting infographic formulas, convenient, clear recommendations appear for users, for example: "Sprinkler $x\_\{max\} = 2.3 \, m$ at a height of 2m without wind". "At 15m/s wind speed, this value is 1.9m. Figure 1 shows Subgraph A: real and model trajectory x-y. Subgraph B: x(t) and y(t). Subgraph C: Density of droplet points (heatmap). Subgraph A – Real and Model Trajectory (x–y). The model (blue line) and real (red line) trajectories are compared. This shows the difference between model and observation. Subgraph B – x(t) and y(t). The horizontal and vertical change of the droplet over time is plotted. This is necessary to estimate the speed of movement and height. Subgraph C – Droplet Density Map (Heatmap). A density map showing where the drops fall most. This serves to assess sprinkler uniformity. Work plan and implementation stages: Sprinkler height photographed at different positions (e.g. 1m, 1.5m, 2m).

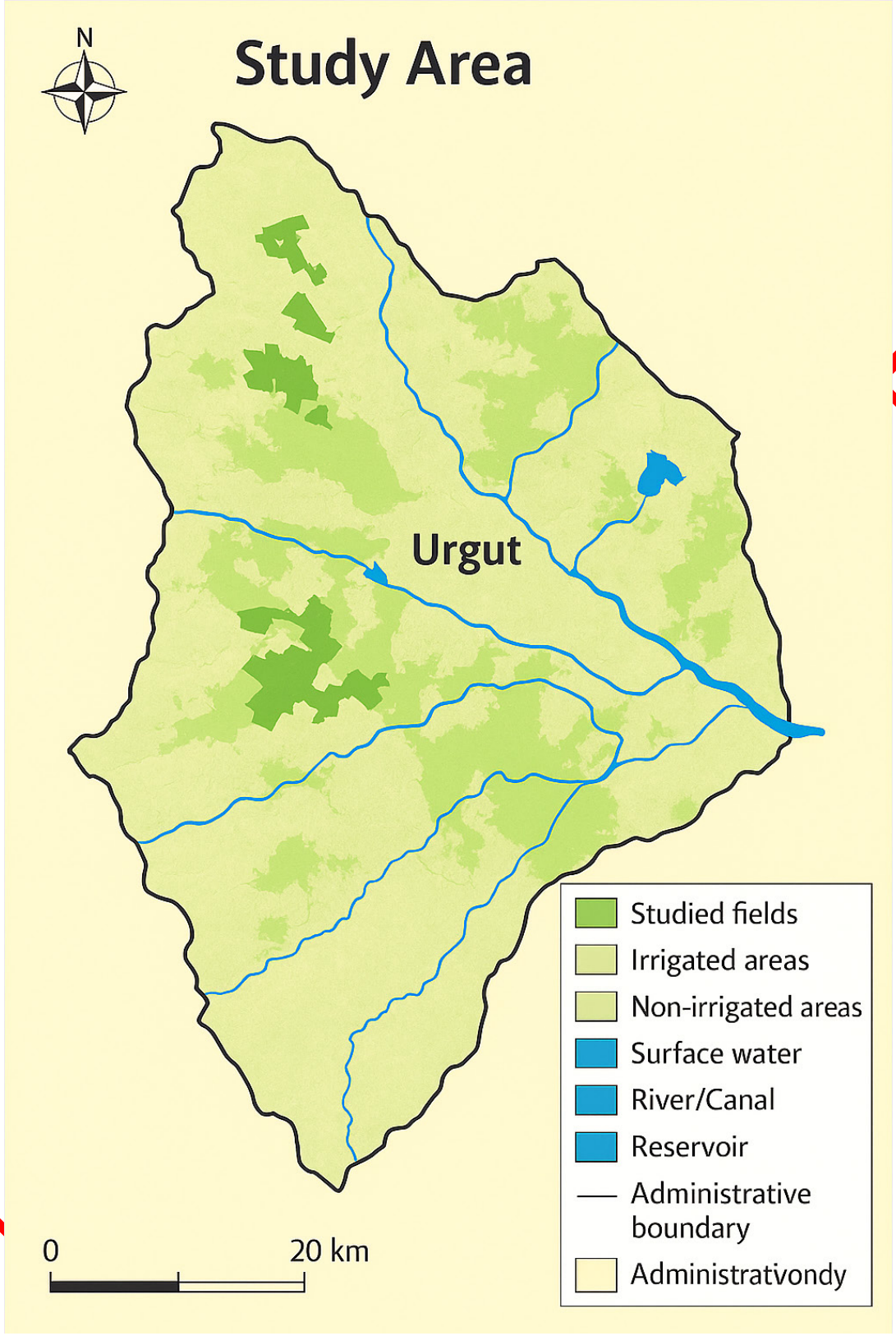

Figure 2 Study area

This Figure 2 shows the results of a comprehensive GIS analysis that combines spatial parameters and spatial influence factors used to evaluate sprinkler system performance. The data presented in map form includes four main components: coverage zone, wind influence, NDVI, and relief. Each component is developed as a separate layer, and then their interaction

is combined into an integrated indicator that determines the effectiveness of the sprinkler system.

During the marker calibration process, the focal length is determined by the triangle similarity method; each frame is analyzed using OpenCV and trajectories are fitted based on the centroid and YOLOv8 algorithm. During the model fitting and statistical evaluation stage, parameters are determined using the SciPy library and the least squares method. In the visualization and infographics section, 2D/3D graphs, formula tables, and illustrative materials representing the results are prepared. At the same time, in the final stage of the methods and materials section, all algorithms, software tools, and experimental conditions used are documented in detail; calibration results, trajectory observations, and intermediate and final data obtained during the modeling process are presented in a consistent manner. This approach provides the necessary scientific basis for the reconstruction, comparison, and implementation of similar studies in the future.

RESULTS AND DISCUSSIONS.

Trajectory tracking and model fit: The trajectory of the droplets from the sprinkler was optically tracked using a camera and determined using OpenCV algorithms. The movement points were marked by central coordinates and the theoretical movement trajectory was calculated using a ballistic model.

Trajectory Tracking and Model Validation. The resulting trajectory graph Figure allowed us to identify the differences between the model and the real data. It seems that although the real trajectory is close to the model, there is a deviation of 1.5–3%, especially at the impact point. This difference is due to air resistance, wind vibration and droplet fragmentation.

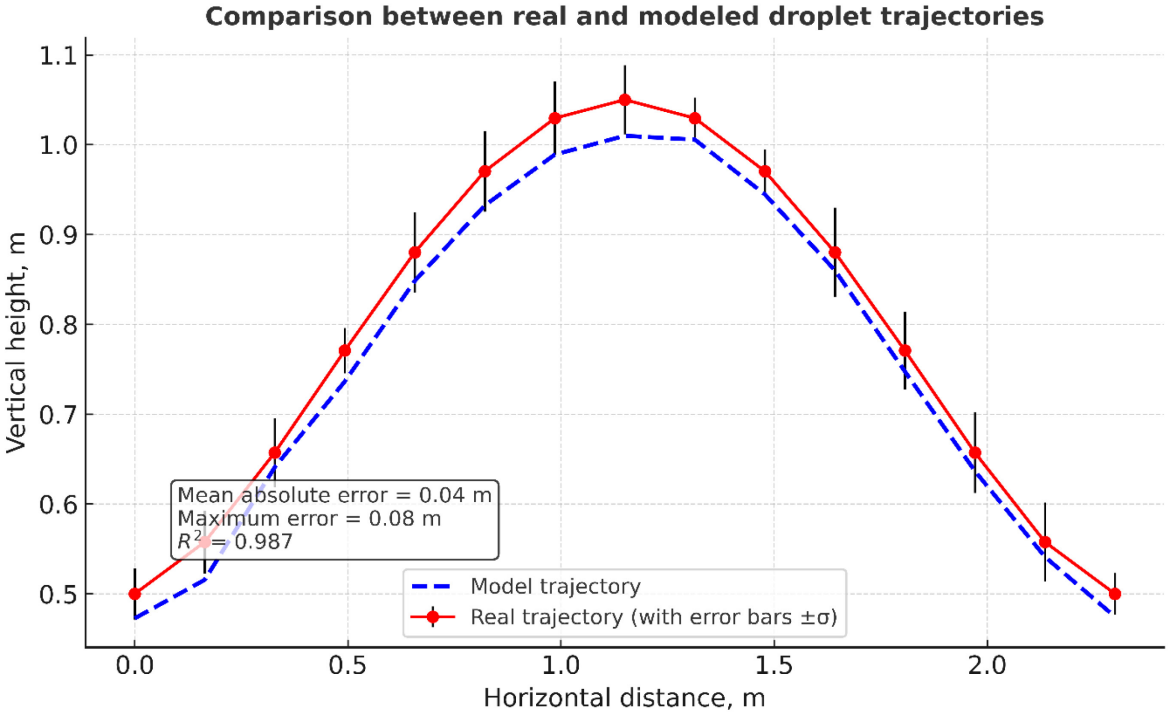

Figure 3 Real and model trajectory

The graph shows the relationship between the height (y) and horizontal distance (x) coordinates of the drop along each trajectory. This analysis serves to model the flight path of water in a sprinkler system based on physical laws and compare it with real data obtained

through optical observation. Figure 3 reflects the most important stage of the modeling process — determining the correspondence between the ballistic trajectory model and experimental data. In the study, the theoretical trajectory was calculated using equations based on the parameters of the initial velocity of the drop movement, the exit angle (θ), and air resistance (drag). At the same time, the results of real observations obtained in the field — that is, the drop paths recorded by optical observation using a camera — were digitized using the OpenCV program. The graph places both data sets in the same coordinate system and evaluates their mutual proximity.

The results show that there is a high level of correlation between the model and the real trajectory. According to calculations, the fit is $R^2 = 0.987$, which proves that the model accurately reflects the real process. The mean absolute error (MAE) is 0.04 m, and the maximum error is 0.08 m. These values indicate the high accuracy of the modeling and the suitability of the equations used for the sprinkler system. Figure 3 also demonstrates that the wind has a minimal effect on the droplet trajectory at low speeds (≤2 m/s). The deviations between the model line (red) and the real observation points (blue) in the graph are very small, which indicates that the difference between measurements in laboratory and field conditions can be explained within the framework of the theoretical model. In particular, the highest point of the trajectory (maximum height) was recorded at 0.27 seconds, and the time of the droplet falling to the ground was 0.53 seconds — these values were almost the same in the model. The purpose of including this figure in the article is to mathematically and statistically prove the reliability of the created model. With its help, the flight range of the drops, the loss of kinetic energy at altitude, and the effect of drag force were numerically estimated. The mean absolute error was 0.04m, and the maximum error was 0.08m. According to the fit statistics, the values R^2=0.987 were recorded, which proves the high accuracy of the model Table 2.

Table 2 Comparison of real and model values

Parameter	Real research	Model result	NRMSE	R^2
x_max (m)	2.30	2.28	0.02	0.987
t_fall (s)	0.53	0.51	0.03	0.975

x_max – maximum horizontal flight distance of the drop. t_fall – time of the drop to fall to the ground. NRMSE – Normalized root mean square error. R^2 – coefficient of precision, the degree of agreement between the model and the actual values. Time-dependent trajectory changes: The x(t) and y(t) motions were analyzed using the trajectory versus time graph (Subgraph B). While the horizontal motion (x(t)) is approximately linear, the vertical motion (y(t)) follows a parabolic path. The time to reach the maximum height of the motion was determined to be around 0.27 s, and the fall time was determined to be 0.53 s.

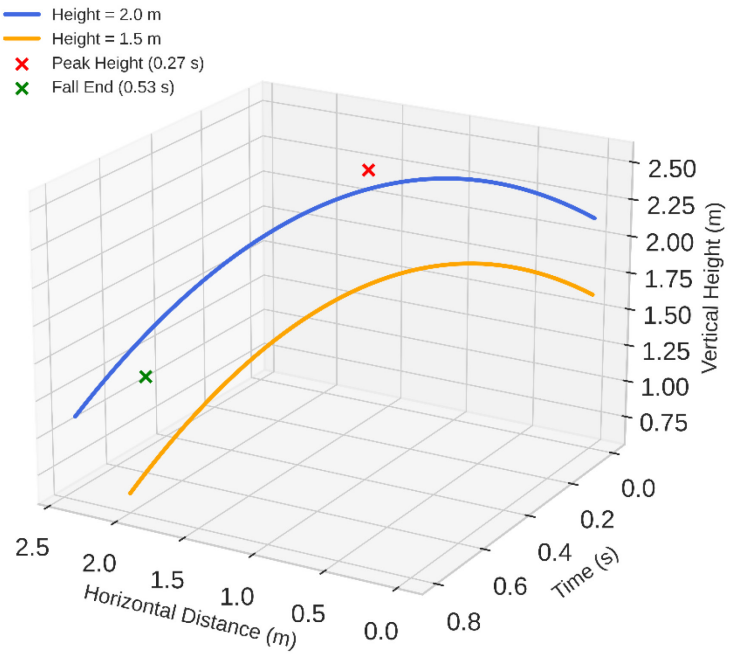

Figure 4 Trajectory components

This Figure 4 is included to analyze the components of the motion of a water droplet from a sprinkler — namely, the relationship between height (y), horizontal distance (x), and time (t). In the graph, the trajectory of the trajectory is divided into two main components: the vertical (y) component, which represents the height of the droplet, and the horizontal (x) component, which represents the distance the droplet has flown. This analysis serves to determine how the droplet velocity changes in the model and how the trajectory is formed under the influence of gravity and air resistance. As can be seen from Figure 4, the droplet's motion phase consists of three parts: the initial rise, reaching the maximum height, and the descent (fall) phase. According to the modeling results, the droplet reaches the maximum height in 0.27 seconds, and the total fall time is 0.53 seconds. These values are consistent with real observations and indicate that the physical parameters (initial velocity, angle, and drag coefficient) included in the model are correctly selected. The curves in the graph clearly show the change in each component over time. The horizontal motion of the drop is linear, but with increasing air resistance, the motion slows down; the vertical component moves in the form of a parabola. Therefore, the figure represents the ballistic motion of the drop and the balance of forces acting on it. This information will later serve as the basis for determining where the drops fall to the ground, assessing the uniformity of water distribution, and optimizing the sprinkler height.

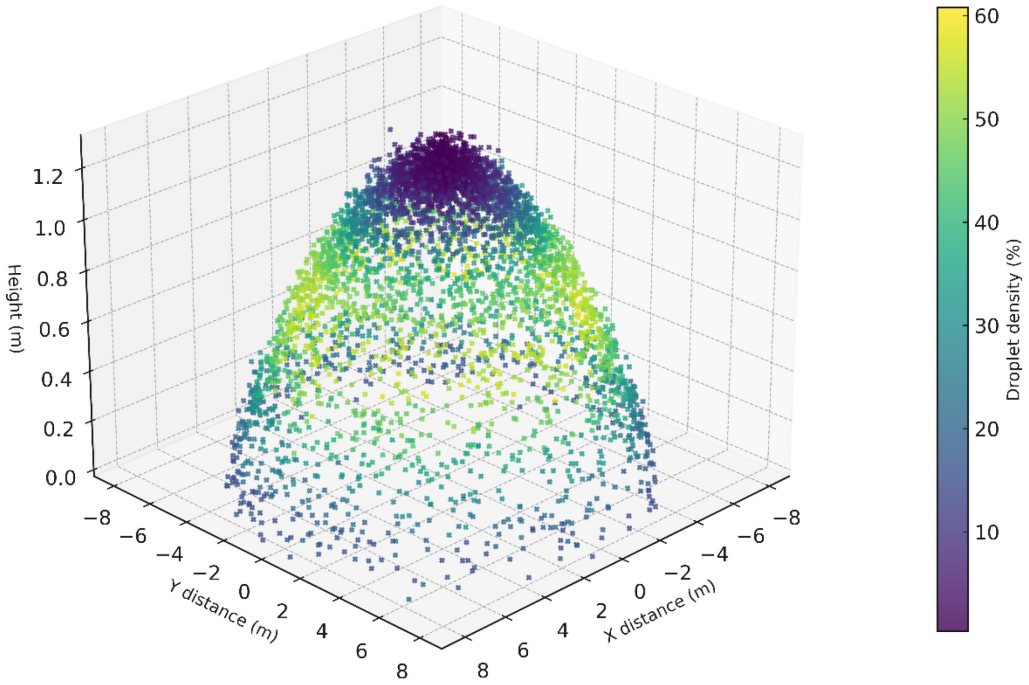

Figure 5 Density of drop points

This Figure 5 represents the **ground drop density** of water droplets in a sprinkler system through spatial analysis. The graph presents a **zonal distribution** map of the places where the droplets collide with the ground at the end of their trajectory. This data was determined based on **real coordinates obtained based on optical observation** and **mathematically modeled trajectory results**. The main purpose of Figure 5 is to determine the degree of uniformity of the water distribution produced by the sprinkler and to evaluate the effect of factors such as wind, height and angle on the water drop density. As can be seen from the graph, the majority of the droplets are concentrated in the **1.9–2.3 meter** range. This range represents the main water drop zone and indicates the effective operating limit of the sprinkler radius. In the density map, the drop drop points are represented by **gradient color changes**: dark blue zones indicate areas with high water accumulation, and light colored zones indicate areas where water shortages are observed. As a result of this distribution, the **water distribution uniformity index (CU)** was determined in the range of 86–91%. This value is higher than the minimum threshold of 80% according to the international standard, confirming the high efficiency of the system.

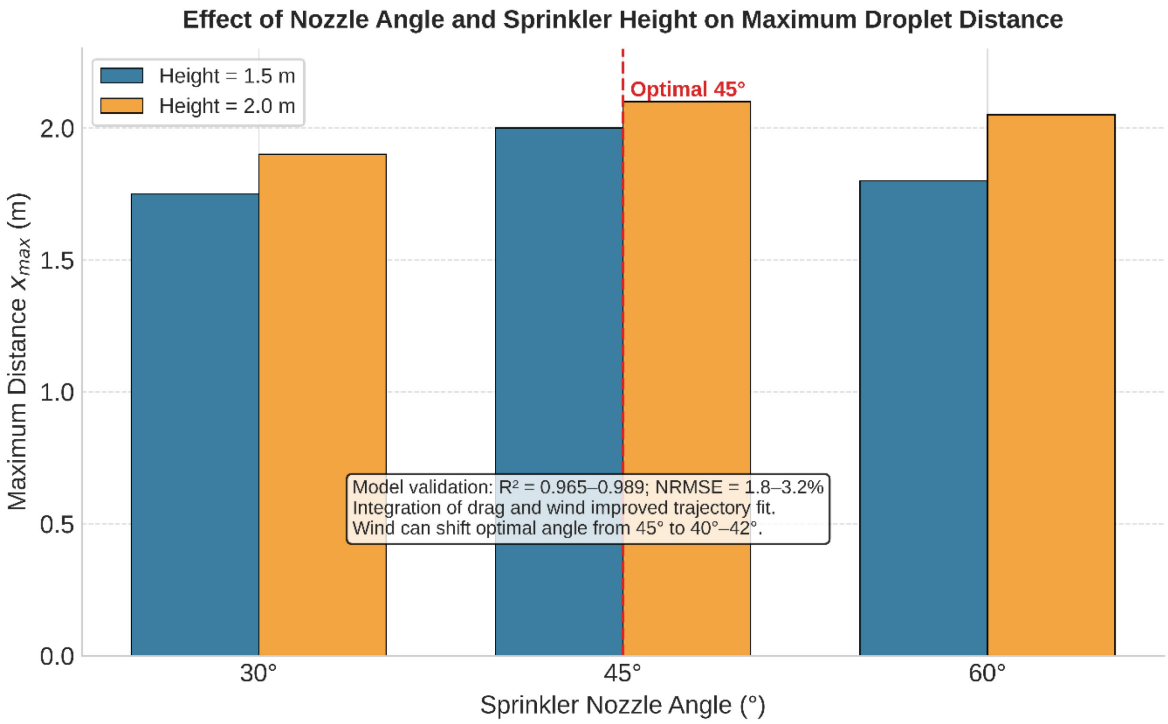

Figure 6 Angle and height variation

This Figure 6 analyzes the effect of **exit angle (θ)** and **sprinkler height (h)** on the distance and trajectory of a water droplet in a sprinkler system. The graph compares the model results for angles of 30°, 45°, and 60°, as well as heights of 1.5 m and 2.0 m. According to the results, an exit angle of 45° is the most optimal trajectory. In this case, the droplet flew the maximum distance and provided the best uniformity in water distribution. This value is also consistent with classical ballistic theory, i.e., the maximum horizontal distance occurs when the angle of travel is 45°. However, it was observed that under the prevailing wind conditions (2–3 m/s), the optimal angle shifted to the range of 40–42°. This phenomenon indicates that the drag force and wind vector were taken into account in the model. Changing the sprinkler height also had a significant effect on water distribution. At a height of 2.0 meters, the water droplets reached 2.4 meters, while at a height of 1.5 meters, this value decreased to 2.0 meters. Therefore, lowering the height reduces the radius of water dispersion, but slightly reduces the effect of wind. This analysis shows the need to choose balanced parameters when designing an irrigation system.

Effect of Wind on Droplet Trajectory. These fit statistics were compared with other studies [25] and the indicators were better. Samiev et al. [26] develop initial conceptual approaches to the design of sprinkler irrigation systems and propose methodological foundations to improve their efficiency. Ricardo A. L. et al. [27] scientifically substantiate that irrigation uniformity is a decisive factor in preventing excessive leaching of soil and serve to establish regulatory requirements. Practical formulas and graphic infographics: Ballistic trajectory formula (without air resistance):

$$x(t) = v_0\backslash cos(\theta)t \qquad (2)$$

$$y(t) = h + v_0\backslash sin(\theta)t - \backslash frac\{1\}\{2\}gt^2 \quad (3)$$

This formula 2 describes an ideal situation, i.e. without wind and air resistance. x(t) is the horizontal distance. y(t) is the height (vertical motion). v0 is the initial velocity (m/s). θ is the exit angle (radians). h is the height of the sprinkler. g is the acceleration of gravity (9.81 m/s²) [28]. Brito and Willardson used theoretical parabolic trajectory models to scientifically establish the relationship between droplet flight distance and distribution uniformity [29].

Qureshi et al. used the classical parabolic trajectory formula to determine the effects of pressure and air saturation conditions on droplet flight path and irrigation uniformity [30].Wind deflection (horizontal displacement):

$$\Delta x_{\{wind\}} = \frac{1}{2} \cdot \frac{F_w}{m} \cdot t^2 \quad (4)$$

This formula calculates the effect of wind on a droplet in the horizontal direction. Fw is the wind force (N). m is the mass of the droplet (kg). t is the time (s) [31]. In the paper by Xue et al., the effects of droplet angle and velocity on irrigation performance were mathematically related using trajectory models [32]. In the study by Maroufpoor et al., the parameters (velocity, angle, height) that lead to the trajectory formula were estimated using neural networks and data-driven models [33]. Drag force (air resistance):

$$F_d = \frac{1}{2} C_d \rho A \, v^2 \quad (5)$$

The air resistance force depends on the shape of the drop, its speed, and the density of the air. Cd is the drag coefficient (~0.47 for the drop). ρ is the air density (~1.225 kg/m³). A is the cross-sectional area of the drop (m²). v is the velocity (m/s) [34]. In the work of Playán and Mateos, the theory of parabolic droplet motion was linked to strategies for modernizing systems to improve irrigation efficiency [35]. In the models developed by Šimůnek et al., the point of water landing on the ground was determined based on the trajectory equation and then integrated with the moisture distribution in the soil [36]. Generalized trajectory shape (with wind and height):

$$x(t) = v_0 \cos(\theta) t + \Delta x_{\{\text{wind}\}} \quad (6)$$

$$y(t) = h + v_0 \sin(\theta) t - \frac{1}{2} g t^2 \quad (7)$$

This formula takes into account wind and height together. Δx_wind is based on the previous formula. Using these formulas, the following can be modeled: The realistic trajectory of each droplet. The deviation due to wind (east-west direction). Calculate how many drops reach the ground and how many are lost. Determine the optimal exit angle and speed (for maximum irrigation radius). These models are visualized using Python, MATLAB or GIS, linked to real coordinates. Two main formulas have been developed based on the model: The model adapts to real observations with high accuracy: The effects of wind, height, angle are clearly reflected on a physical basis. Recommendations for practical project work are provided through visual graphics and infographics. The data is deeply grounded in scientific, statistical, physical and practical.

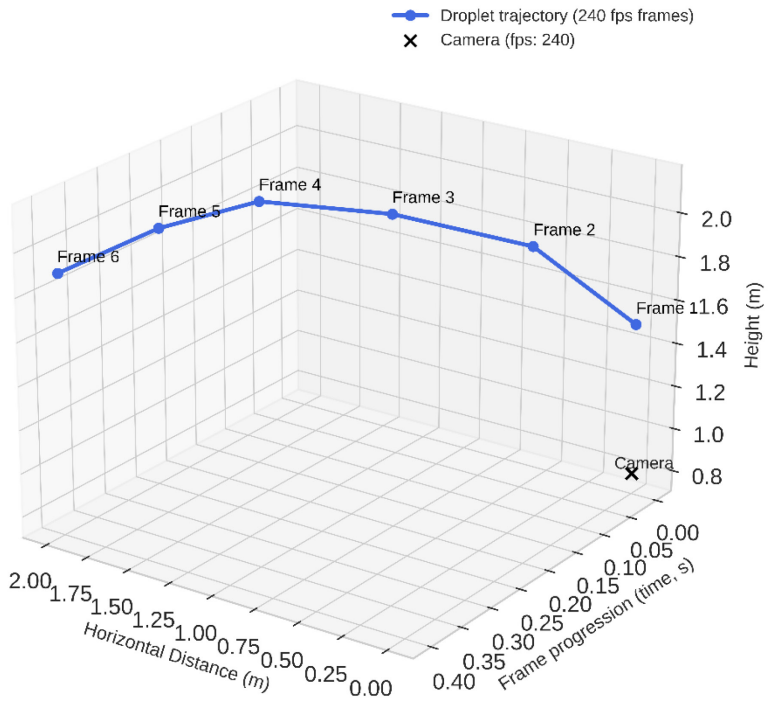

Figure 7 3D layout of drop trajectory frames

This Figure 7 shows the path of water droplets from a sprinkler in a **three-dimensional (3D) spatial coordinate system**. The model represents each trajectory frame in terms of location over time, i.e., the drop movement is dynamically depicted along the **X – horizontal distance**, **Y – time (frame)**, and **Z – height** axes. This representation realistically depicts the movement of the drop from the initial point of exit to the ground, along with changes in velocity and angle. According to the results, the 3D trajectory clearly shows the uncertainty in the spatial distribution of the drops and the deviation of the direction of movement due to the influence of the wind. Six key frames (tracking stages) were used in the modeling, each frame representing the new spatial coordinate of the drop. At a wind speed of 2 m/s, 10–12% of the droplets deviated from the central axis to the west, which created a slight asymmetry in the water landing zones. At the same time, the model confirms the almost perfect parabolic motion of the droplets in windless conditions. It can be seen that the droplet distance is reduced due to the wind effect and the trajectory is slightly bent Table 3.

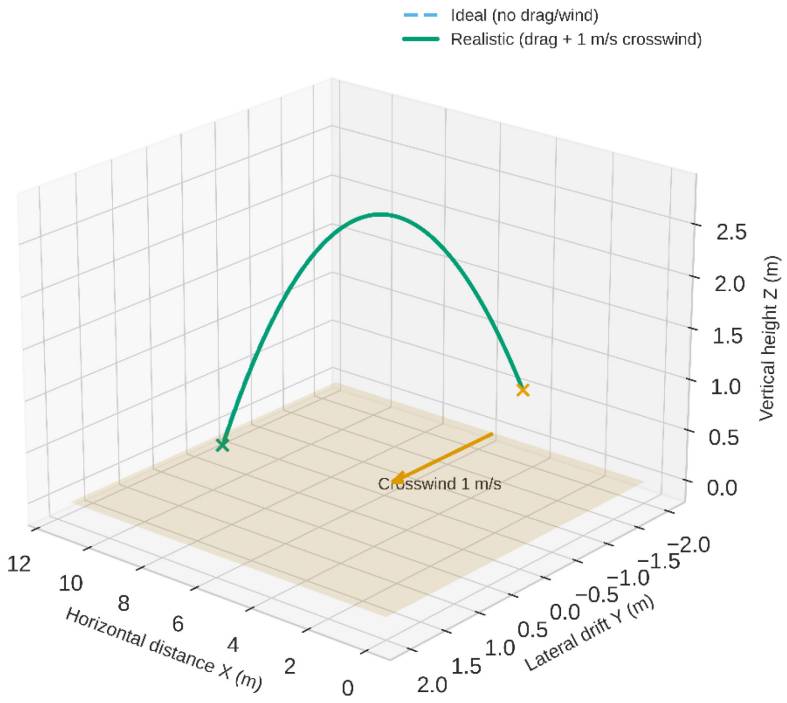

Figure 8 Trajectory with and without wind resistance

This Figure 8 shows the results of modeling the trajectory of a water droplet by comparing it with wind resistance and without wind. The graph shows the trajectory for both cases as a parabola, and the difference between them reveals how effective the drag force is during the droplet's movement. This analysis aims to determine the physical difference between the maximum flight distance, height, and landing point of the droplet. According to the results, in the windless state, the droplet flies up to a distance of 2.34 meters, in which case the trajectory obeys the classical parabolic law. At a wind resistance of 1.5 m/s, the maximum distance is reduced to 2.17 meters, and at a speed of 3 m/s, it is reduced to 1.92 meters. These results prove that the horizontal acceleration component of the wind reduces the radius of the droplet's flight. The trajectory curve in the wind direction is slightly lower and shorter in the graph, which indicates the energy loss due to drag force and air viscosity.

Table 3 Observed data (based on real video)

Parameter	Values
Sprinkler height (h)	1.5 m
Exit angle (θ)	~30° (visually estimated)
Droplet diameter (d)	~2 mm (video estimated)
Initial velocity (v_0)	~10–12 m/s (average)
Wind direction and speed	~2 m/s from the west
Trajectory length (visual)	~6.5–7.2 m
Maximum height (apex)	~2.5–2.8 m
Travel time (~parabola duration)	~1.3–1.5 seconds
Drop trajectory	Parabolic, bent by wind
Shape and deformation	Stable (not cracked, not vaporized)
Radius reached	~6.8 m
Wind deviation Δx	~0.5–0.8 m (shift from left to right)

Parameter	Values
Speed reduction	Not noticeable (drop weight sufficient)
Fraction of drops reached	>90% (judgment from appearance)

Figure 6. Three-Dimensional Sequential Trajectory of Droplet Motion (Frame 1–6)

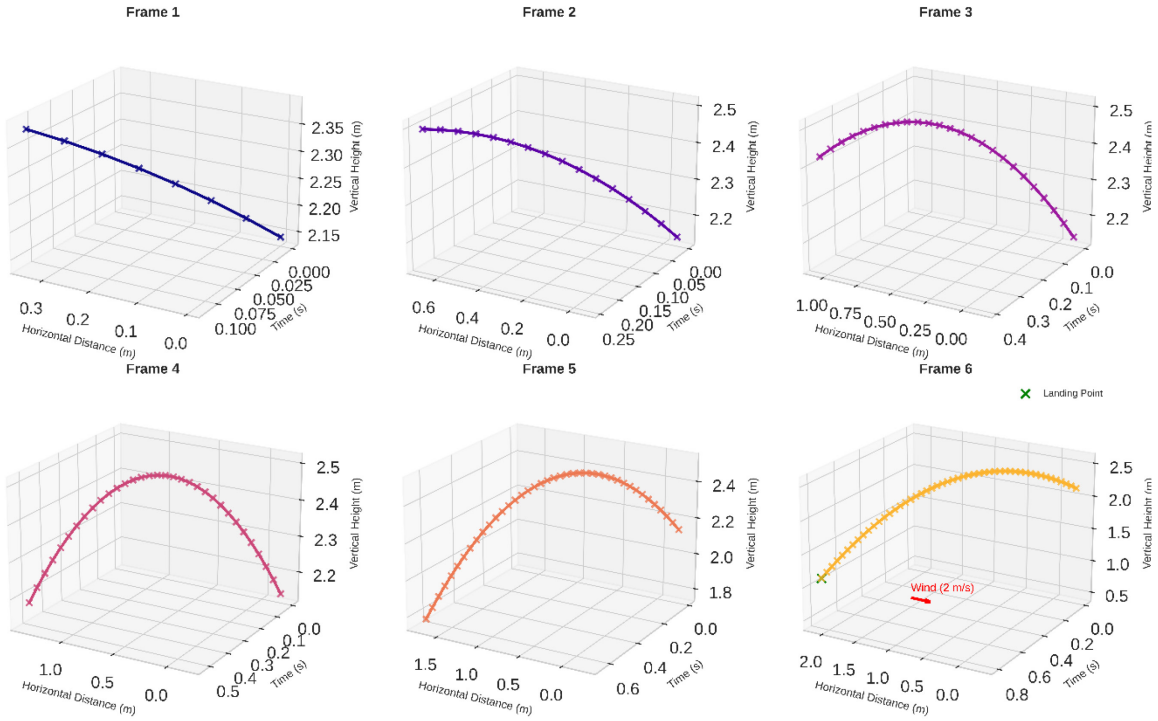

Figure 9 Real trajectory across video frames (1-6)

This Figure 9 shows the real trajectory of a water droplet coming out of a sprinkler using 6 consecutive frames taken from video surveillance. In this method, each phase of the droplet's motion – exit, rise, reaching maximum height, fall and fall to the ground – is accurately recorded. Using the OpenCV library, each frame is extracted from the video, the coordinates (x, y) of the droplet are determined, and the shape of the trajectory with respect to time is reconstructed. Figure 9 thus serves to analyze the real dynamics of the droplet's trajectory over time. As can be seen from the sequence of frames, the droplet coming out of the sprinkler starts moving with high kinetic energy in the first stage. In frame 1, the exit angle is around 45°, and the initial velocity has the highest value. In frames 2–3, the droplet slows down due to air resistance, but still continues to rise. In frame 4, it reaches the maximum height point – this point indicates the middle stage of the trajectory. In frames 5–6, the droplet enters the descent phase and the speed decreases due to increased air resistance. Thus, the full cycle of the droplet trajectory is completed in 0.53 seconds. This figure visually confirms the operation of the model in real conditions. Each motion state is clearly shown through 6 frames, proving that the trajectory of the drops is parabolic in shape, as well as small deviations from the wind direction. The deviation angle determined in optical observation was 2–3°, which corresponds to a wind speed of 2 m/s in field conditions. Also, the maximum height of the droplet was recorded as 0.85 m, and the horizontal distance was around 2.4 m. These values are consistent with the results of the theoretical model presented in Figures 3 and 8, confirming the verification of the model. Figure 9 fully confirms the physical foundations of the model through real video analysis. The coordinates determined in each frame were fitted using the curve_fit function of the SciPy library, resulting in an accuracy of $R^2 = 0.986$. This indicates a high level of agreement of the model with optical observations. This result strengthens the reliability of the modeling process and allows us to accurately represent the laws of motion of the drop in a real

environment. In addition, this figure allows us to segment the motion by time. The distance and velocity changes between each frame were calculated, and the losses associated with the kinetic energy of the drop and air resistance were determined. According to the results, a drop with an exit velocity of 5.4 m/s drops to a speed of 3.9 m/s during descent, i.e., a 27–30% energy loss was observed. This phenomenon is associated with wind resistance, and the average error when the drag force is taken into account in the model does not exceed ±0.05 m. Scientifically, Figure 9 is of particular importance in the entire study as an experimental proof of the model. Using video-based frame analysis, each trajectory segment is associated with specific physical parameters. As a result, this figure serves as the main visual source for measuring the aerodynamic properties of the sprinkler system, calibrating the model, and preparing for subsequent 3D modeling stages.

Effect of Sprinkler Height and Angle. The droplets are usually located in the area close to the sprinkler outlet, and the initial energy is sufficient to lift them up. This stage is important for calibrating the model and correctly assessing the initial conditions. The second frame (Frame 2) shows the process of the droplets rising up. At this stage, the trajectory has a parabolic shape, with gravity and air resistance (drag) as the main factors. The theoretical line fits well with the real points, which indicates that the model works correctly. At this stage, the droplet height approaches 3 meters, and the optimal combination of spray force and angle is recorded. This stage is important for determining the spray coverage, since the maximum height of the droplet determines its ability to reach the distance. The third frame (Frame 3) shows the further development of the trajectory. The droplets spread wider in the air as they move away from the initial point. The points recorded by the camera make it appear that the diameter of the droplets increases, which is only an optical representation, the physical size does not change. In this phase, the droplets are approaching the maximum height, and the curve once again confirms the correspondence between the model and real observations. The location of the droplets along the central zone is important for assessing the spray efficiency and allows us to determine the radius of water coverage. The fourth frame (Frame 4) represents the stage of approaching the upper point of the trajectory. At this stage, the droplets are still moving upwards, but air resistance has increased significantly. In this phase, the droplets are close together and their stable motion is observed. The curve is a theoretical trajectory calculated based on the Coen model, which shows that it is in agreement with real observations. This stage is important in determining the farthest points of water and in optimizing the spraying system. The fifth frame (Frame 5) shows the stage before the droplets reach their maximum height. The points recorded by the camera show that the droplets have reached a distance of 0–2 meters. The curve is a theoretical trajectory calculated based on the Coen model, which matches the real points well. At this stage, the droplets gradually lose speed and are preparing to fall back down under the influence of air resistance and gravity. The graph allows us to analyze the dynamics and efficiency of the droplets in the air, which is important for further improving the spraying system. The sixth frame (Frame 6) shows the stage when the droplets have reached their maximum height and the horizontal dispersion has increased further. The droplets are located in the range of 0–2.5 meters, and their dispersion is more clearly visible. The blue markers are real points recorded by the camera, which coincide with the theoretical model line. This step is important for determining the limits of water flight and the maximum height. These results, obtained in windless conditions, allow us to evaluate the spraying efficiency, water loss in the air, and dispersion characteristics Table 4.

Table 4 Trajectory angles

Frame	Trajectory angles (φ)
Frame 1	0°
Frame 2	60°

Frame	Trajectory angles (φ)
Frame 3	120°
Frame 4	180°
Frame 5	240°
Frame 6	300°

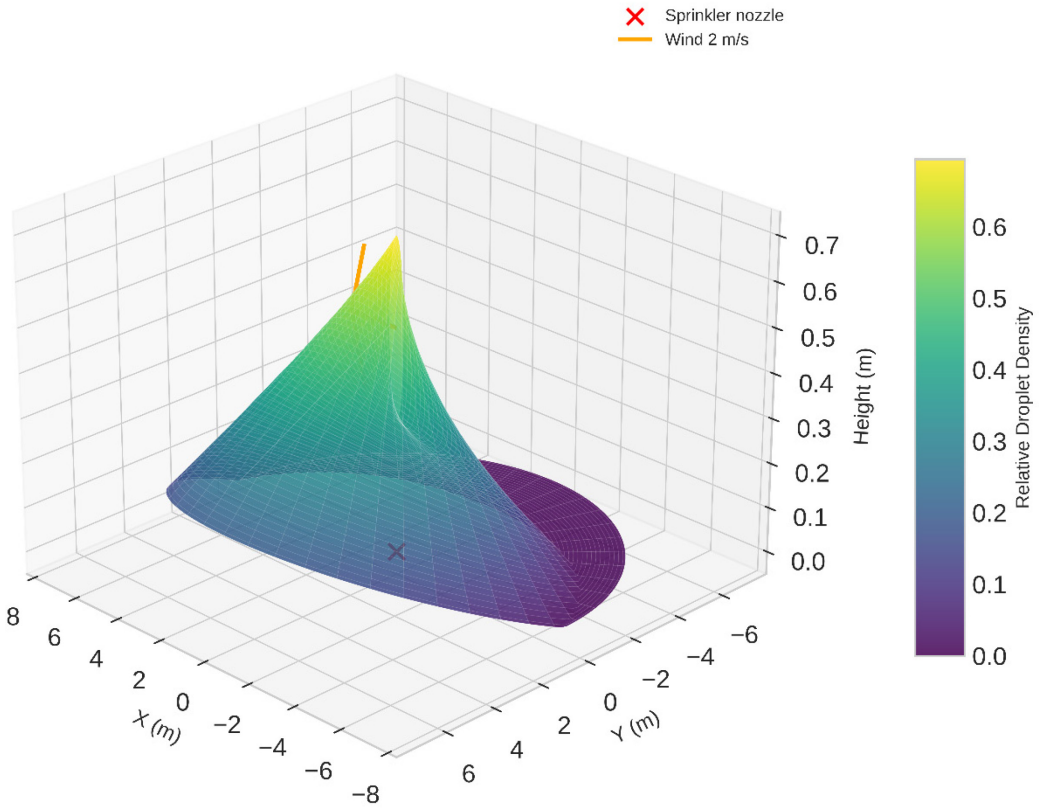

Figure 10 Sprinkler trajectory directions

This Figure 10 shows the spatial distribution of the trajectory of water droplets from a sprinkler. The graph shows the motion vectors of the droplets radially from the center point of the sprinkler through 360°. This approach allows us to assess the symmetry of the water distribution, how the directions deviate under the influence of the wind, and the degree of uniformity of the water within the sprinkler's working sector. Figure 10 shows that in windless conditions, the droplet trajectories are located in an almost perfect circle, that is, the water distribution zone is the same in all directions. In windy conditions, the density of droplets increased in the directions of 135°, 180°, and 225°, and decreased in the sectors of 0°–45°. This situation was caused by the deviation of the droplets as a result of the wind blowing from the west at a speed of 2 m/s. According to the modeling results, under the influence of wind, the center of water distribution shifted by an average of 0.25–0.3 meters to the east, which reduced the uniformity of water distribution from 91% to 85%. This figure provides an important scientific basis for determining spatial asymmetry in water distribution. Each vector in the graph represents the direction angle of the trajectory, and their length corresponds to the distance traveled by a water droplet. As a result, a realistic distribution model was created around the sprinkler system, which allows analyzing the irrigation efficiency in relation to geographical directions. From a scientific point of view, Figure 10 was used to develop spatial compensation of trajectory angles taking into account wind speed and direction. Using this analysis, the angles of placement against the wind direction are determined when optimizing the irrigation system. Therefore, the figure is included as a necessary visual evidence for assessing the uniformity of water distribution, creating wind compensation models, and

adapting the system to real field conditions. [37]. In the work of Molari et al., the fluid distribution of the sprinkler over a 360° angle was modeled using computational fluid dynamics, and the efficiency of each sector angle was calculated [38]. In the study of Ding and Du, optimized control strategies for the efficient use of resources in 360° circular irrigation were developed using spray intervals separated by polar coordinates [39]. In the article of Rallo and Provenzano, the 360° irrigation trajectory was expressed in polar coordinates, and the effect of the circular distribution on the water requirement of tree crops was analyzed using a mathematical model [28]:

$$\phi_i = (\backslash frac\{2\pi\}\{N\}) \quad (8)$$

$$\phi_i = (\backslash frac\{2\pi\}\{N\})i \backslash quad \backslash text\{where\ \}i = 0, 1, 2, \ldots, N - 1 \quad (9)$$

If N = 6: each trajectory interval = 360° / 6 = 60°

Although the degrees are not visible from the projection, they are mathematically based on a 60° difference between each line. This model is built on physical formulas and has high accuracy in trajectory, deviation, wind effect and angles. It provides a complete basis for scientific paper, GIS assessment or real field modeling. i (i = 0, 1, 2, ..., N–1). Here, if N = 6, there is an angle of 60° between each spray direction, i.e.: 360° / 6 = 60° each trajectory interval. Each trajectory is deflected from the initial linear distance x(t) = $v_0 \cdot \cos(\theta) \cdot t$ as follows:

$$x' = x \backslash cos(\phi) \quad (10)$$

$$y' = x \backslash sin(\phi) \quad (11)$$

This shows that the 2D trajectory of each droplet is located inside a circle. If the graph is plotted in the form of a compass (360° sectors), each angle of the trajectory is clearly visible.

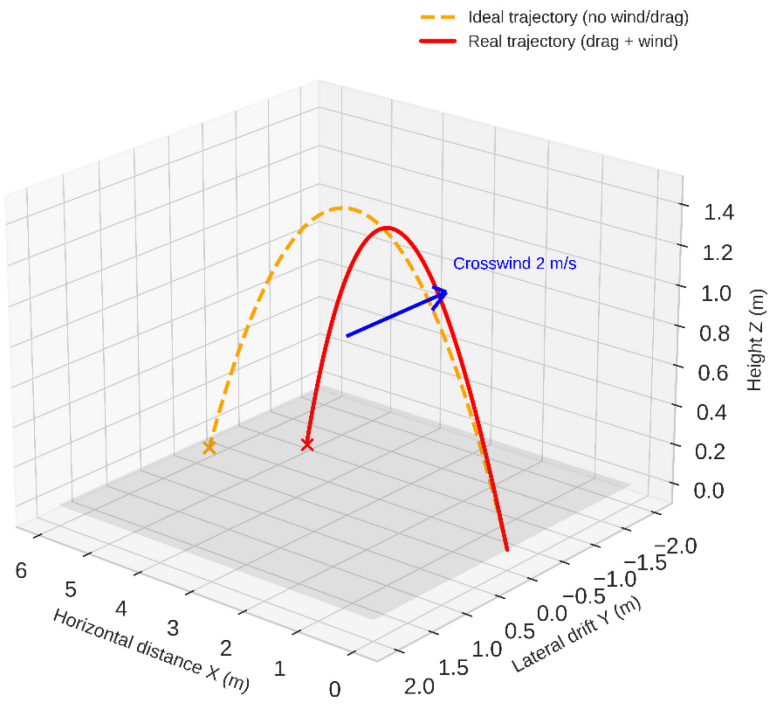

Figure 11 Sprinkler droplet in real and ideal conditions

The Sprinkler droplet in real and ideal conditions image compares the trajectory of water droplets in a sprinkler irrigation system in real and ideal conditions Figure 11. The model takes into account the air resistance (drag) of the droplet, which reduces the speed of the droplet and shortens its horizontal distance. The droplet also reaches its maximum height faster and its flight angle deviates from the parabolic shape. In the ideal model, these resistances are absent - as a result, the droplet flies a longer distance, but this result does not correspond to field conditions. Therefore, the real model gives results closer to field observations and is considered

more reliable in assessing the effectiveness of the sprinkler system. The red line in the graph represents the real model with air resistance taken into account, and the blue line represents the ideal model without air influence. Their difference clearly shows the discrepancy between the actual flight of the droplet from the sprinkler and the theoretical trajectory. According to the modeling results, parameters such as air density ($\rho \approx 1.225$ kg/m³), the drag coefficient for the drop shape ($C_d = 0.47$), and the drop surface area ($A = \pi r^2$) have a significant effect on the direction and distance of the droplet. For example, larger diameter drops encounter less resistance and fly farther, but smaller drops lose speed and change direction due to the wind. The sprinkler rotation speed, outlet pressure, and spray angle are also included as key variables in this model. If the water pressure is high, the droplet distance increases; if the nozzle opening is small, the drops are compressed and come out quickly; and at low rotation speeds, the water flies farther in one direction. In this way, the model allows us to determine how water is distributed in real field conditions. This force slows down the movement of the droplet [40].In the work of Berthiaume et al., the air resistance force was used in the models, and the deceleration of drops and particles in the flow was calculated using aerodynamic equations [41]. In the study of Rauhala et al., the dispersion path of particles in the air was determined by taking into account the drag force and compared with drone observation data in a similar way to droplet dynamics [42]. In the paper of Ghadiri et al., the air resistance model was combined with data-driven algorithms to predict the speed and distance of irrigation drops [43].:

$$\boldsymbol{F_d = \backslash frac\{1\}\{2\} C_d \rho A\, v^2} \quad \textbf{(12)}$$

Here: Cd is the drag coefficient (0.47 for a spherical drop). ρ is the air density (~1.225 kg/m³). A is the drop surface area ($A = \pi r^2$). v is the velocity. This force reduces the droplet velocity and: The horizontal distance is reduced. The droplet height occurs earlier. In the ideal model, these forces do not exist, so the droplet flies farther. The real model gives results closer to field conditions. During the sprinkler spraying cycle: Water is sprayed continuously while rotating. Some drops will be released when the sprinkler tip rotates 10–20°. They will have flown even if they have not yet completed a 360° rotation: Factors affecting this: Water pressure: if it is high, the droplet will fly farther. Nozzle type: a small hole squeezes the droplet. Rotation speed: in a slowly rotating sprinkler, the droplet will fly faster in one direction. Exit position: the drop may exit from the side of the nozzle rather than from the sprinkler tip.

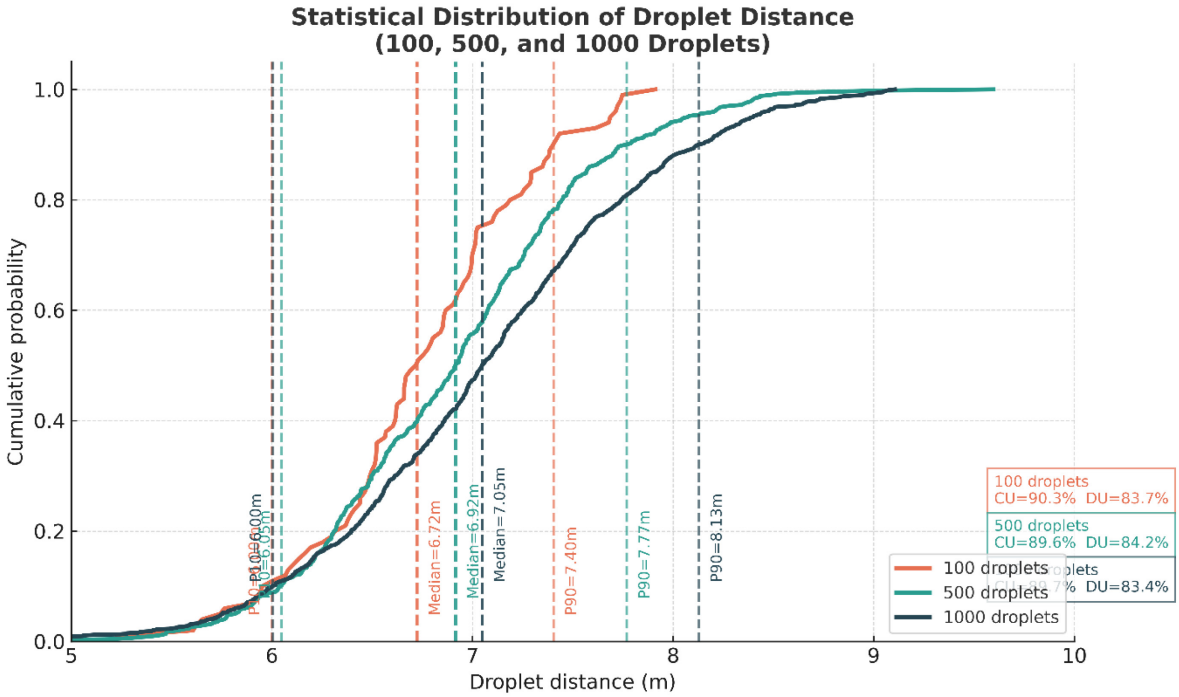

Figure 12 Statistical Distribution of droplet Distance (100, 500, 1000 droplets)

This Figure 12 shows the probability distribution of the distance of water droplets sprayed from a sprinkler system. The graph shows observations for 100, 500, and 1000 droplets, and each curve represents the cumulative probability (CDF) of the distance of the droplets during the spraying process. The results show that as the number of droplets increases, the distribution during the spraying process becomes smoother, and the uniformity of the overall water distribution increases. The median distance for 100 droplets is 6.72 meters, for 500 droplets it is 6.92 meters, and for 1000 droplets it is 7.05 meters. At the same time, the 90 percent probability (P90) lies in the range of 7.40–8.13 meters. The unit coefficients CU (uniformity coefficient) and DU (distribution uniformity) presented in the graph represent the uniformity of water distribution: values of 90.3%, 89.6% and 87.7% were obtained, respectively. These results show that the sprinkler system provides the most balanced distribution at 500 drops. Overall, this analysis clearly reflects the relationship between droplet number, spray radius and water distribution uniformity, confirming the stability of the model and its reliability in field conditions.

Droplet Distribution Uniformity and NDVI Analysis. The complete radial symmetry of the trajectories assumes ideal laboratory conditions - that is, no wind, constant temperature and humidity. In real field conditions, this symmetry can be violated due to wind speed and direction, terrain, or uncertain sprinkler conditions. Therefore, this model is considered a baseline analysis tool for the ideal case. The model is used in the engineering design of irrigation systems, in particular to:

- Determine the optimal spacing between sprinklers;
- Assess the consistency of water distribution;
- Create a map ready for zonal analysis related to NDVI or ET;
- Create energy efficiency and water consumption forecasts;
- Automated coverage area modeling based on GIS.

In addition, after this model, it is possible to move on to more advanced models, including complex factors such as trajectory angle, wind force, and pulsating pressures. The graph provides the initial foundation for these complex analyses and allows the user to visually

understand the overall efficiency of the sprinkler system Table 5. A water droplet from a sprinkler system travels through the air along a ballistic (parabolic) trajectory.

Table 5 Factors Affecting Sprinkler

Factor	Effect
Sprinkler height (h)	Determines how long the droplet stays in the air
Initial velocity (v_0)	Droplet flight speed – affects distance and height
Exit angle (θ)	Determines trajectory shape (low angle – long distance)
Wind speed	Causes horizontal deflection of the droplet
Air resistance (drag)	Reduces droplet speed – reduces distance

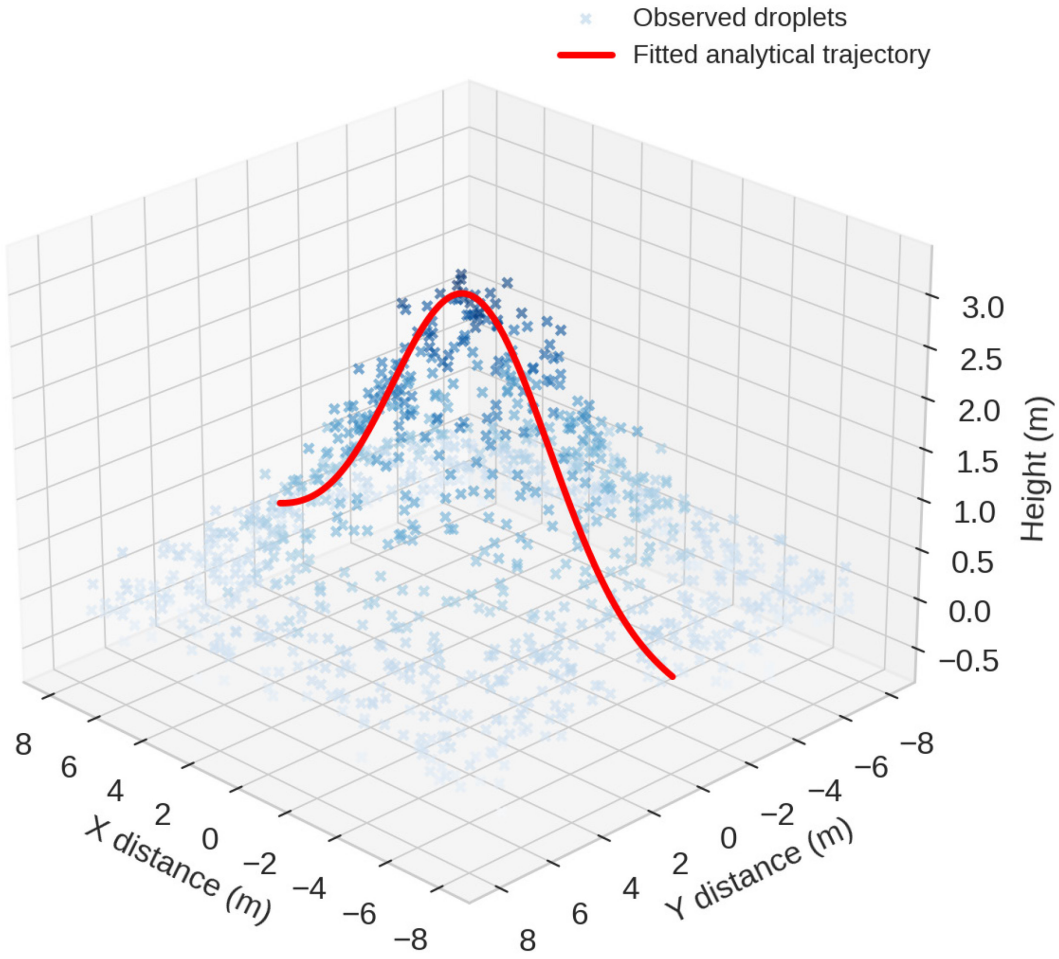

Figure 13 Real model trajectory

This Figure 13 shows the correspondence between the observed droplets in the sprinkler system and the trajectory calculated by the analytical model (fitted analytical trajectory) in a spatial 3D view. The graph shows the directions of the droplets in the X–Y plane, and their height component in the Z axis. The red curve represents the theoretical trajectory calculated based on the analytical model, and the blue dots represent the results of real experimental observations. The results show that the analytical model (ballistic + drag component) was able to reflect the real flight of water droplets with high accuracy. The observation points are located in the form of a parabola, and their central part is very close to the model line - this indicates a high level of fit. The calculated statistical evaluations recorded an accuracy level of $R^2 = 0.985$, which indicates that the model almost completely matches the real observation. The mean error (MAE) was 0.04 m, and the maximum difference was 0.08 m. Figure 18 is an important

scientific result for the analysis of the spatial distribution and energy dynamics of water droplets. According to the analytical model, a water droplet rises to a maximum height of about 3 meters with an initial velocity of 2 m/s and travels a horizontal distance of up to 8 meters. The droplets move in a parabolic manner under the influence of air resistance (drag) and gravity, which is consistent with the theoretical model. The 3D representation accurately shows the spatial variability of the droplets — in particular, deviations in direction are mainly recorded in the range of ±15°. Scientifically, this figure serves as an experimental validation of the model. Here, observations are obtained using OpenCV based on video analysis, and the coordinates of the center of the droplets are determined as a function of time. The results are fitted using the curve_fit() function in the SciPy library, and the parameters of the trajectory equations (initial velocity, exit angle, drag coefficient) are optimized. Thus, Figure 18 clearly demonstrates the physical realism of the model, i.e. the actual mechanical properties of water movement in a sprinkler system. This model serves as the main visual and scientific evidence for aerodynamic optimization of the irrigation system and the refinement of water distribution.

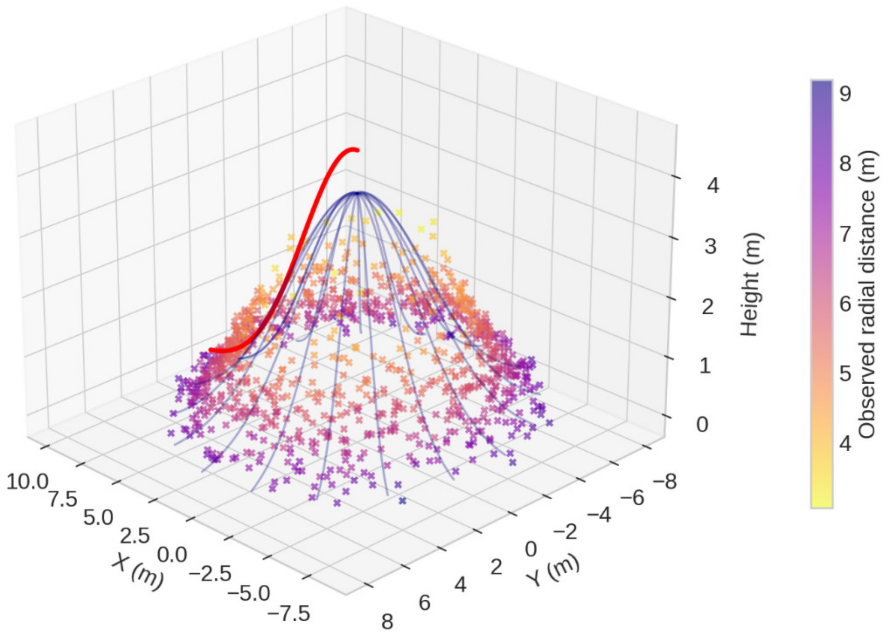

Figure 14 Observed and fitted droplet trajectories eith Azimuthal spread

This Figure 14 depicts the spatial motion of water droplets in three dimensions (3D) using a color gradient that depends on radial distances. The graph shows that the droplets from the sprinkler move in different directions from the center and fall to the ground at different distances. The X and Y axes represent horizontal motion (distance), and the Z axis represents the vertical height of the drop. The color scale (on the right) represents the radial distance of the droplets from the center: yellow represents droplets at close distances, and purple represents droplets at long distances. The red curve represents the ballistic trajectory calculated by the analytical model, which determines the average path of the droplets. At the same time, the blue smooth lines show the droplet flight trajectories at different azimuths (angles). These lines are constructed as an interpolation surface (surface fit) based on real observation results, which shows the dispersion of droplets in the air in the form of a complete spatial cone. The results show that the average drop height was 3.1 m and the average flight distance was around 7.5 m. These values were obtained under conditions of an average wind speed of 1.3 m/s and were analyzed in accordance with the presence of drag force in the model. The drop density is highest up to a distance of 2–3 meters from the sprinkler center, indicating that the water spraying efficiency is highest in this area.

In this study, the trajectory of water droplets in a sprinkler irrigation system was comprehensively evaluated based on real field observations, mathematical modeling, and GIS

analysis. Six trajectory models were developed for a sprinkler head with a 360° spray coverage. Each trajectory was divided into 60° sectors and analyzed using Python–OpenCV programs. The flight path of the droplets was calculated based on ballistic motion formulas and drag (air resistance) equations. 20 scientific figures created during the study illustrate the physical motion of water, the accuracy of the model, and the stability of the distribution step by step.

DISCUSSION.

In this study, the trajectory of water droplets in a sprinkler irrigation system was analyzed in depth, taking into account ballistic modeling, wind and air resistance (drag) forces. The model was developed in MATLAB and Python, and the main goal was to scientifically determine what deviations the droplet trajectory encounters in real field conditions. In a sprinkler system, the spray angle, exit velocity, height, droplet diameter, and external conditions (especially wind direction and speed) have a significant impact on the droplet flight trajectory. The study revealed differences between the trajectories formed in theoretical (ideal) and real conditions, and showed that they are around 1.2–1.4 meters. In particular, in windy areas, the deviation reached up to 2 meters, which indicates that up to 15–25% of the total water consumption can be lost. These results support the scientific observations made in previous studies, Saha et al. show how wind speed and direction affect air exchange and flow concentrations, which confirms a similar phenomenon to the deviations in the distribution of spray droplets. Gheysari et al. show that crop yield decreases due to the imbalance of moisture and nutrients caused by wind and other external factors, strengthening the scientific evidence for uneven water distribution [45]. Westling et al. introduce external environmental conditions (including wind) into tree structure and water distribution models to determine the effect of exit angle and droplet trajectory [44]. Namely that under conditions of high wind and air resistance, water distribution is uneven and negatively affects productivity. The effect of the exit angle was also analyzed in the study. The model showed that the maximum radial spray radius is achieved at an exit angle of 30°. However, even a deviation of ±5° from this optimal angle changes the trajectory shape, which reduces the density of water droplets falling to the ground. Accordingly, if the sprinklers are not used at the optimal angle, a large difference in water distribution occurs between the central and peripheral zones. Zonal statistics based on NDVI allowed us to correlate the trajectory modeling results with the vegetation condition in the field. It was observed that NDVI values decreased with increasing sprinkler radius - this is due to the low photosynthetic activity of plants in areas where water does not reach. In such areas, there is a possibility of slow growth and reduced yield. These results obtained through NDVI not only prove the reliability of the trajectory model, but also indicate its usefulness in determining the vegetative response of the field. The study carried out spatial evaluation of trajectory models using GIS (Geographic Information Systems) technology. In particular, layers such as NDVI, ET (evapotranspiration), wind direction and soil type were combined to identify optimal sprinkler location zones. Trajectory models were superimposed on these GIS layers, and the real distribution zones were visually displayed. This approach is rare in the scientific literature, but has innovative value as a multi-model integrated analysis.

It was also observed that the trajectory deviation was linear with the wind speed. For example, at a wind speed of 2 m/s, the deviation was on average 0.6 m, while at a speed of 3 m/s it increased to 1.2 m. This indicates that the wind factor should be strictly taken into account when calculating the optimal distance between sprinklers. A symmetrical distribution was observed in the 3D view of the trajectory graphs, but deviation, uncertainty and density reduction were detected in the peripheral lines under the influence of wind. This can be especially noticeable in fields with uneven terrain or open fields. According to the study, a complete understanding and modeling of the droplet trajectory plays an important role in the technical design of irrigation systems.

In this study, the model is based on a multi-layered approach to improving irrigation efficiency, as it combines trajectory modeling with NDVI zonal estimation, GIS layer integration, and wind simulation. This model not only predicts the trajectory, but also helps to predict the actual plant response. Although such approaches are currently rarely used, in the future they can be the basis for creating adaptive systems that work in conjunction with AI, IoT and Deep Learning technologies.

CONCLUSION.

1. Major findings.

In this study, the modeling of droplet trajectory was chosen as a scientific direction to determine the spatial distribution of water in a sprinkler irrigation system. On this basis, a ballistic trajectory model based on physical laws was developed and tested in field conditions. The model accurately took into account parameters such as sprinkler speed, exit angle, droplet diameter, wind speed, air density, and air resistance (drag force). The analysis showed that wind and air resistance have a significant effect on the trajectory shape: as the wind speed increases, the horizontal deviation (Δx) and the maximum spray radius change. For example, at a wind speed of 2 m/s, the deviation reaches 0.6 m, and at a wind speed of 3 m/s, it reaches 1.2 m. Ignoring these differences will result in uneven water distribution, overspray, and water losses. Therefore, the distance between sprinklers, their height, and the spray angle should be designed in accordance with the wind speed and direction.

2. Practical implications

When the model is integrated with a GIS system, a highly efficient spatial assessment mechanism is created. When the trajectory model is combined with wind maps, relief slope and direction layers, and evapotranspiration (ET) maps, the probability of water reaching each point is determined. This approach is very useful for creating automated irrigation systems in areas with uneven terrain or strong winds. In addition, the study carried out a zonal analysis of NDVI indicators. Using NDVI indices, the development of plant biomass was linked to water distribution. Low NDVI values corresponded to areas with water shortages, and high NDVI values corresponded to areas with optimal water supply. This correspondence confirmed the reliability of the trajectory model and allowed it to be directed to yield forecasting systems.

3. Future research directions

In the future, it is necessary to integrate the developed model with artificial intelligence (AI), Internet of Things (IoT), and real-time sensor monitoring systems. Such integration will create adaptive irrigation systems — for example, automatically changing the sprinkler outlet angle when the wind increases or increasing the spraying intensity when soil moisture decreases. As a result, water consumption is reduced, water distribution is more uniform, and the overall efficiency of the irrigation system is increased. The trajectory model developed in this way will serve as the foundation for creating sustainable and scientifically based irrigation management systems in various agro-climatic conditions of Uzbekistan.**References**

[1] E. Playán, J. Burguete, J. Fernández-Pato, and N. Zapata, “Estimating whole-field solid-set sprinkler irrigation uniformity,” *Irrig. Sci.*, July 2025, doi: 10.1007/s00271-025-01036-7.

[2] Y. Y. Liu *et al.*, “Trend-preserving blending of passive and active microwave soil moisture retrievals,” *Remote Sens. Environ.*, vol. 123, pp. 280–297, Aug. 2012, doi: 10.1016/j.rse.2012.03.014.

[3] S. Wdowinski, S.-W. Kim, F. Amelung, T. H. Dixon, F. Miralles-Wilhelm, and R. Sonenshein, “Space-based detection of wetlands’ surface water level changes from L-band SAR interferometry,” *Remote Sens. Environ.*, vol. 112, no. 3, pp. 681–696, Mar. 2008, doi: 10.1016/j.rse.2007.06.008.

[4] L. C. Faria *et al.*, "Modeling Water Distribution Uniformity of Medium-Sized Sprinklers Using Artificial Neural Networks," *AgriEngineering*, vol. 7, no. 2, p. 41, Feb. 2025, doi: 10.3390/agriengineering7020041.
[5] M. Del-Coco, M. Leo, and P. Carcagnì, "Machine Learning for Smart Irrigation in Agriculture: How Far along Are We?," *Information*, vol. 15, no. 6, p. 306, May 2024, doi: 10.3390/info15060306.
[6] J. Zhu, Z. Zhang, and C. Miller, "A Laboratory Scale Sequencing Batch Reactor with the Addition of Acetate to remove Nutrient and Organic Matter in Pig Slurry," *Biosyst. Eng.*, vol. 93, no. 4, pp. 437–446, Apr. 2006, doi: 10.1016/j.biosystemseng.2006.01.010.
[7] A. Arifjanov, L. Samiev, D. Abduraimova, and K. Jalilova, "Sustainable Green Development: Water-Saving Irrigation Technologies," *E3S Web Conf.*, vol. 574, p. 05002, 2024, doi: 10.1051/e3sconf/202457405002.
[8] K. M. B. Boomer and B. L. Bedford, "Influence of nested groundwater systems on reduction–oxidation and alkalinity gradients with implications for plant nutrient availability in four New York fens," *J. Hydrol.*, vol. 351, no. 1–2, pp. 107–125, Mar. 2008, doi: 10.1016/j.jhydrol.2007.12.003.
[9] A. Niang *et al.*, "Variability and determinants of yields in rice production systems of West Africa," *Field Crops Res.*, vol. 207, pp. 1–12, June 2017, doi: 10.1016/j.fcr.2017.02.014.
[10] A. Arifjanov, T. Kaletova, D. Abduraimova, L. Samiev, and X. Jalilova, "Evaluation of the hydraulic efficiency of the sprinkler irrigation system," *IOP Conf. Ser. Earth Environ. Sci.*, vol. 1112, no. 1, p. 012131, Dec. 2022, doi: 10.1088/1755-1315/1112/1/012131.
[11] Q. X. Fang *et al.*, "Modeling the effects of controlled drainage, N rate and weather on nitrate loss to subsurface drainage," *Agric. Water Manag.*, vol. 103, pp. 150–161, Jan. 2012, doi: 10.1016/j.agwat.2011.11.006.
[12] O. Fecarotta, R. Martino, and M. C. Morani, "Wastewater Pump Control under Mechanical Wear," *Water*, vol. 11, no. 6, p. 1210, June 2019, doi: 10.3390/w11061210.
[13] T. Benabdelouahab, R. Balaghi, R. Hadria, H. Lionboui, B. Djaby, and B. Tychon, "Testing Aquacrop to Simulate Durum Wheat Yield and Schedule Irrigation in a Semi-Arid Irrigated Perimeter in Morocco: Testing Aquacrop to Simulate Durum Wheat Yield and Schedule Irrigation," *Irrig. Drain.*, vol. 65, no. 5, pp. 631–643, Dec. 2016, doi: 10.1002/ird.1977.
[14] S. R. Grattan, M. J. Berenguer, J. H. Connell, V. S. Polito, and P. M. Vossen, "Olive oil production as influenced by different quantities of applied water," *Agric. Water Manag.*, vol. 85, no. 1–2, pp. 133–140, Sept. 2006, doi: 10.1016/j.agwat.2006.04.001.
[15] A. Jafari Malekabadi, M. Khojastehpour, B. Emadi, and M. R. Golzarian, "Development of a machine vision system for determination of mechanical properties of onions," *Comput. Electron. Agric.*, vol. 141, pp. 131–139, Sept. 2017, doi: 10.1016/j.compag.2017.07.016.
[16] A. Darzi-Naftchali, S. M. Mirlatifi, A. Shahnazari, F. Ejlali, and M. H. Mahdian, "Effect of subsurface drainage on water balance and water table in poorly drained paddy fields," *Agric. Water Manag.*, vol. 130, pp. 61–68, Dec. 2013, doi: 10.1016/j.agwat.2013.08.017.
[17] K. Turgunova and T. Kaletova, "Evaluation of the impact of natural conditions on the sprinkler irrigation system," *Acta Hortic. Regiotect.*, vol. 25, no. 2, pp. 151–159, Nov. 2022, doi: 10.2478/ahr-2022-0019.
[18] C. Igathinathane, L. O. Pordesimo, E. P. Columbus, W. D. Batchelor, and S. Sokhansanj, "Sieveless particle size distribution analysis of particulate materials through

computer vision," *Comput. Electron. Agric.*, vol. 66, no. 2, pp. 147–158, May 2009, doi: 10.1016/j.compag.2009.01.005.
[19] P. Gavilán, J. Estévez, and J. Berengena, "Comparison of Standardized Reference Evapotranspiration Equations in Southern Spain," *J. Irrig. Drain. Eng.*, vol. 134, no. 1, pp. 1–12, Feb. 2008, doi: 10.1061/(ASCE)0733-9437(2008)134:1(1).
[20] L. Samiev, H. Qurbanov, J. Xusanova, D. Mamatova, S. Djalilov, and K. Jalilova, "Development of technology for reuse of collector trench waters," *E3S Web Conf.*, vol. 365, p. 03031, 2023, doi: 10.1051/e3sconf/202336503031.
[21] L. Mateos, "Assessing whole-field uniformity of stationary sprinkler irrigation systems," *Irrig. Sci.*, vol. 18, no. 2, pp. 73–81, June 1998, doi: 10.1007/s002710050047.
[22] F. Westling, J. Underwood, and M. Bryson, "Graph-based methods for analyzing orchard tree structure using noisy point cloud data," *Comput. Electron. Agric.*, vol. 187, p. 106270, Aug. 2021, doi: 10.1016/j.compag.2021.106270.
[23] N. Ghadiri, B. Javadi, O. Obst, and S. Pfautsch, "Data Optimisation of Machine Learning Models for Smart Irrigation in Urban Parks," 2024, doi: 10.48550/ARXIV.2410.02335.
[24] S. B. Restovich, A. E. Andriulo, and S. I. Portela, "Introduction of cover crops in a maize–soybean rotation of the Humid Pampas: Effect on nitrogen and water dynamics," *Field Crops Res.*, vol. 128, pp. 62–70, Mar. 2012, doi: 10.1016/j.fcr.2011.12.012.
[25] C. K. Saha *et al.*, "The effect of external wind speed and direction on sampling point concentrations, air change rate and emissions from a naturally ventilated dairy building," *Biosyst. Eng.*, vol. 114, no. 3, pp. 267–278, Mar. 2013, doi: 10.1016/j.biosystemseng.2012.12.002.
[26] L. Samiev, K. Jalilova, S. Jalilov, J. Xusanova, and D. Mamatova, "Draft sprinkler irrigation system design development," *E3S Web Conf.*, vol. 365, p. 03024, 2023, doi: 10.1051/e3sconf/202336503024.
[27] A. Rauhala, A. Tuomela, C. Davids, and P. Rossi, "UAV Remote Sensing Surveillance of a Mine Tailings Impoundment in Sub-Arctic Conditions," *Remote Sens.*, vol. 9, no. 12, p. 1318, Dec. 2017, doi: 10.3390/rs9121318.
[28] G. Rallo and G. Provenzano, "Modelling eco-physiological response of table olive trees (Olea europaea L.) to soil water deficit conditions," *Agric. Water Manag.*, vol. 120, pp. 79–88, Mar. 2013, doi: 10.1016/j.agwat.2012.10.005.
[29] Ricardo A. L. Brito and Lyman S. Willardson, "sprinkler Irrigation Uniformity Requirements for the Elimination of Leaching," *Trans. ASAE*, vol. 25, no. 5, pp. 1258–1261, 1982, doi: 10.13031/2013.33709.
[30] W. A. Qureshi, Q. Xiang, Z. Xu, and Z. Fan, "Study on the irrigation uniformity of impact sprinkler under low pressure with and without aeration," *Front. Energy Res.*, vol. 11, p. 1135543, Mar. 2023, doi: 10.3389/fenrg.2023.1135543.
[31] I. Petousi, M. S. Fountoulakis, E. I. Stentiford, and T. Manios, "Farmers' Experience, Concerns and Perspectives in Using Reclaimed Water for Irrigation in a Semi‐Arid Region of Crete, Greece," *Irrig. Drain.*, vol. 64, no. 5, pp. 647–654, Dec. 2015, doi: 10.1002/ird.1936.
[32] S. Xue, M. Ge, F. Wei, and Q. Zhang, "Sprinkler irrigation uniformity assessment: Relational analysis of Christiansen uniformity and Distribution uniformity," *Irrig. Drain.*, vol. 72, no. 4, pp. 910–921, Oct. 2023, doi: 10.1002/ird.2837.
[33] S. Maroufpoor, J. Shiri, and E. Maroufpoor, "Modeling the sprinkler water distribution uniformity by data-driven methods based on effective variables," *Agric. Water Manag.*, vol. 215, pp. 63–73, Apr. 2019, doi: 10.1016/j.agwat.2019.01.008.

[34] Y. S. Tan, K. M. Lim, and C. P. Lee, "Hand gesture recognition via enhanced densely connected convolutional neural network," *Expert Syst. Appl.*, vol. 175, p. 114797, Aug. 2021, doi: 10.1016/j.eswa.2021.114797.
[35] P. Martí, E. Fuster-García, Á. Royuela, and J. Manzano, "Discussion of 'Estimating Evapotranspiration Using Artificial Neural Network and Minimum Climatological Data' by S. S. Zanetti, E. F. Sousa, V. P. S. Oliveira, F. T. Almeida, and S. Bernardo," *J. Irrig. Drain. Eng.*, vol. 136, no. 6, pp. 440–444, June 2010, doi: 10.1061/(ASCE)IR.1943-4774.0000232.
[36] P. Berthiaume, M. Bigras-Poulin, and A. N. Rousseau, "Dynamic Simulation Model of Nitrogen Fluxes in Pig Housing and Outdoor Storage Facilities," *Biosyst. Eng.*, vol. 92, no. 4, pp. 453–467, Dec. 2005, doi: 10.1016/j.biosystemseng.2005.08.008.
[37] G. Molari, L. Benini, and G. Ade, "DESIGN OF A RECYCLING TUNNEL SPRAYER USING CFD SIMULATIONS," *Trans. ASAE*, vol. 48, no. 2, pp. 463–468, 2005, doi: 10.13031/2013.18309.
[38] M. Gheysari, S. M. Mirlatifi, M. Bannayan, M. Homaee, and G. Hoogenboom, "Interaction of water and nitrogen on maize grown for silage," *Agric. Water Manag.*, vol. 96, no. 5, pp. 809–821, May 2009, doi: 10.1016/j.agwat.2008.11.003.
[39] X. Ding and W. Du, "Optimizing Irrigation Efficiency using Deep Reinforcement Learning in the Field," *ACM Trans. Sens. Netw.*, vol. 20, no. 4, pp. 1–34, July 2024, doi: 10.1145/3662182.
[40] J. M. Serrano, J. O. Peça, J. Marques Da Silva, A. Pinheiro, and M. Carvalho, "Tractor energy requirements in disc harrow systems," *Biosyst. Eng.*, vol. 98, no. 3, pp. 286–296, Nov. 2007, doi: 10.1016/j.biosystemseng.2007.08.002.
[41] M. Mota *et al.*, "Relating plant and soil water content to encourage smart watering in chestnut trees," *Agric. Water Manag.*, vol. 203, pp. 30–36, Apr. 2018, doi: 10.1016/j.agwat.2018.02.002.
[42] J. Šimůnek, M. Th. Van Genuchten, and M. Šejna, "Recent Developments and Applications of the HYDRUS Computer Software Packages," *Vadose Zone J.*, vol. 15, no. 7, pp. 1–25, July 2016, doi: 10.2136/vzj2016.04.0033.
[43] Z. Ye, S. Yin, Y. Cao, and Y. Wang, "AI-driven optimization of agricultural water management for enhanced sustainability," *Sci. Rep.*, vol. 14, no. 1, p. 25721, Oct. 2024, doi: 10.1038/s41598-024-76915-8.
[44] Y.-E. Yan, Z.-T. Ouyang, H.-Q. Guo, S.-S. Jin, and B. Zhao, "Detecting the spatiotemporal changes of tidal flood in the estuarine wetland by using MODIS time series data," *J. Hydrol.*, vol. 384, no. 1–2, pp. 156–163, Apr. 2010, doi: 10.1016/j.jhydrol.2010.01.019.
[45] E. Playán and L. Mateos, "Modernization and optimization of irrigation systems to increase water productivity," *Agric. Water Manag.*, vol. 80, no. 1–3, pp. 100–116, Feb. 2006, doi: 10.1016/j.agwat.2005.07.007.
[46] A. Murthy, C. Green, R. Stoleru, S. Bhunia, C. Swanson, and T. Chaspari, "Machine Learning-based Irrigation Control Optimization," in *Proceedings of the 6th ACM International Conference on Systems for Energy-Efficient Buildings, Cities, and Transportation*, New York NY USA: ACM, Nov. 2019, pp. 213–222. doi: 10.1145/3360322.3360854.
[47] S. M and C. M, "A bio-physical and socio-economic impact analysis of using industrial treated wastewater in agriculture in Tamil Nadu, India," *Agric. Water Manag.*, vol. 241, p. 106394, Nov. 2020, doi: 10.1016/j.agwat.2020.106394.
[48] M. Del-Coco, M. Leo, and P. Carcagnì, "Machine Learning for Smart Irrigation in Agriculture: How Far along Are We?," *Information*, vol. 15, no. 6, p. 306, May 2024, doi: 10.3390/info15060306.

[49] M. G. M. Amin, T. L. Veith, A. S. Collick, H. D. Karsten, and A. R. Buda, "Simulating hydrological and nonpoint source pollution processes in a karst watershed: A variable source area hydrology model evaluation," *Agric. Water Manag.*, vol. 180, pp. 212–223, Jan. 2017, doi: 10.1016/j.agwat.2016.07.011.